Monthly Notices
of the
ROYAL ASTRONOMICAL SOCIETY

MNRAS **474,** L7–L11 (2018)
Advance Access publication 2017 December 6

doi:10.1093/mnrasl/slx189

Jet-driven and jet-less fireballs from compact binary mergers

O. S. Salafia,[1,2,3]★ G. Ghisellini[2] and G. Ghirlanda[2]

[1] *Univ. di Milano Bicocca, Dip. di Fisica 'G. Occhialini', Piazza della Scienza 3, I-20126 Milano, Italy*
[2] *INAF – Osservatorio Astronomico di Brera, via E. Bianchi 46, I-23807 Merate, Italy*
[3] *INFN – Sezione di Milano-Bicocca, Piazza della Scienza 3, I-20126 Milano, Italy*

Accepted 2017 November 12. Received 2017 November 8; in original form 2017 October 1

ABSTRACT

During a compact binary merger involving at least one neutron star (NS), a small fraction of the gravitational energy could be liberated in such a way to accelerate a small fraction ($\sim 10^{-6}$) of the NS mass in an isotropic or quasi-isotropic way. In presence of certain conditions, a pair-loaded fireball can form, which undergoes accelerated expansion reaching relativistic velocities. As in the standard fireball scenario, internal energy is partly transformed into kinetic energy. At the photospheric radius, the internal radiation can escape, giving rise to a pulse that lasts for a time equal to the delay time since the merger. The subsequent interaction with the interstellar medium can then convert part of the remaining kinetic energy back into radiation in a weak isotropic afterglow at all wavelengths. This scenario does not require the presence of a jet: the associated isotropic prompt and afterglow emission should be visible for all NS–NS and BH–NS mergers within 90 Mpc, independent of their inclination. The prompt emission is similar to that expected from an off-axis jet, either structured or much slower than usually assumed ($\Gamma \sim 10$), or from the jet cocoon. The predicted afterglow emission properties can discriminate among these scenarios.

Key words: gravitational waves – relativistic processes – gamma-ray burst: general – stars: neutron.

1 INTRODUCTION

The detection and identification of an electromagnetic (EM) counterpart to a gravitational wave (GW) event is the next fundamental step for assessing the properties of the progenitors, refine the distance inferred from the GW signal alone and improve our general understanding of these phenomena.

Black hole–black hole (BH–BH) mergers likely produce no EM signature (even though some possibilities have been proposed, see e.g. Loeb 2016; Perna, Lazzati & Giacomazzo 2016; Yamazaki, Asano & Ohira 2016). We are left with neutron star–neutron star (NS–NS) or black hole–neutron star (BH–NS) mergers. These are the long foreseen progenitors of Short Gamma Ray Bursts (SGRBs), whose typical observed (isotropically equivalent) radiated energy is around $E_{\rm iso} \sim 10^{51}$ erg, with a typical spectral peak energy $E_{\rm peak} \sim 0.1$–1 MeV (e.g. D'Avanzo et al. 2014). The SGRB emission is thought to be produced by a relativistic, collimated jet of half-opening angle $\theta_{\rm jet} \sim 5$–15 degrees (Berger 2014; Troja et al. 2016). If the jet bulk Lorentz factor Γ is large, say $\Gamma \gtrsim 100$, this implies that we can detect only the small fraction $f_b = (1 - \cos\theta_{\rm jet}) \sim 10^{-2}$–$10^{-3}$ of SGRB jets that are observed within the half-opening angle (i.e. with a viewing angle $\theta_{\rm view} \leq \theta_{\rm jet}$).

If the jet is *structured*, with Γ (and/or the energetics) decreasing with increasing angular distance from the jet axis, we have somewhat better chances to see the SGRB prompt emission at large viewing angles (e.g. Pescalli et al. 2015; Salafia et al. 2015; Kathirgamaraju, Barniol Duran & Giannios 2017).

In order to reach relativistic velocity, the jet must excavate its way through the merger (dynamical) and post-merger (disc-viscosity-driven and neutrino-driven) ejecta, which may pollute significantly the environment ahead the formation of the jet (Just et al. 2016; Murguia-Berthier et al. 2017). In doing so, the jet deposits part of its energy in a cocoon, which may produce a quasi-isotropic prompt, high-energy EM signal soon after the merger by photospheric release of relic thermal photons (the 'cocoon prompt emission' – Lazzati et al. 2017b, 2017a) possibly followed, on a time-scale of hours, by UV/optical emission powered by nuclear-decay and cooling (the 'cocoon UV emission' – Gottlieb, Nakar & Piran 2018) and, on a time-scale of days, by synchrotron emission upon interaction of the expanding cocoon with the interstellar medium (ISM) (the 'cocoon afterglow' – Lazzati et al. 2017a). The energy the jet deposits in the cocoon is of the order of $\sim 10^{49}$ erg. For the cocoon prompt emission, Lazzati et al. (2017a) predict a short ($\sim$1 s) signal with an energy of $\sim 10^{46}$– 10^{47} erg peaking at $\sim$10 keV.

The possibilities just mentioned (structured jet and energized cocoon) both require the presence of a jet. In this letter, we investigate the possibility to have a detectable isotropic emission in hard

★ E-mail: omsharan.salafia@gmail.com

X-rays in NS–NS and BH–NS mergers *without* a jet. We are guided by the fact that isolated magnetars can produce giant flares with $E_{\rm iso} \sim 10^{46}$ erg (e.g. Hurley et al. 2005; Lazzati, Ghirlanda & Ghisellini 2005) in non-catastrophic events, probably due to some re-configuration of their magnetic field (Thompson & Duncan 1995). In NS–NS and BH–NS mergers, the gravitational energy available during the last phase of the coalescence is more than $E_{\rm G} \sim 10^{53}$ erg, and only a very small fraction of this needs to be used.

To explore this possibility, we postulate that a small fraction (e.g. less than 0.1 per cent) of $E_{\rm G}$ can be used, e.g. through magnetic field amplification and subsequent conversion of magnetic field energy into thermal and/or kinetic energy, during the initial phase of the coalescence. The magnetic field in the NS material during the merger reaches values larger than $B \sim 10^{15}$ G (Price 2006; Zrake & MacFadyen 2013; Kiuchi et al. 2014; Giacomazzo et al. 2015; Ruiz & Shapiro 2017). This is enough to form a fireball, which can produce an important isotropic emission in hard X-rays, as first suggested by Zrake & MacFadyen (2013) and Giacomazzo et al. (2015).

Various recent numerical simulations (e.g. Just et al. 2016; Murguia-Berthier et al. 2017; Ruiz & Shapiro 2017) and theoretical works (e.g. Margalit, Metzger & Beloborodov 2015) suggest that the conditions for launching a relativistic jet after a NS–NS or BH–NS merger are not always satisfied, thus the fraction of mergers without jets might be significant. The possible presence of a prompt, isotropic, high-energy component is thus particularly relevant for what concerns the prospects for future associations of EM counterparts to nearby GW events: the other most promising candidate EM counterpart so far, which is the nuclear-decay-powered emission from the merger and post-merger ejecta (the so-called *kilonova*; Li & Paczyński 1998; Metzger 2017), is predicted to emit in the optical and near-infrared, where no all-sky monitoring instruments are available to date.

2 SET-UP OF THE ISOTROPIC FIREBALL MODEL

The binding energy difference between an isolated NS and a BH of the same mass is

$$\Delta E_{\rm G} \sim \frac{3}{10} M_{\rm NS} c^2 \left(1 - \frac{R_{\rm S}}{R_{\rm NS}}\right) \sim 5 \times 10^{53}\,{\rm erg}, \quad (1)$$

where $R_{\rm S}$ is the Schwarzschild radius, $M_{\rm NS}$ and $R_{\rm NS}$ are the mass and radius of the NS, respectively, and the numerical value is for $M_{\rm NS} = 1.4\,{\rm M}_\odot$ and $R_{\rm NS} = 14\,{\rm km}$.

This energy is of the same order as that released in a supernova explosion. In that case, most of it goes into neutrinos. In a compact binary merger, it powers several other processes, such as emission of GWs, dynamical ejection of matter and magnetic field amplification. The latter process is widely believed to produce a magnetic field of the order of $B \sim 10^{15}$–10^{16} G (Price 2006; Zrake & MacFadyen 2013; Kiuchi et al. 2014; Giacomazzo et al. 2015; Ruiz & Shapiro 2017), which in turn can contain an energy of the order of $\sim 10^{51}$ erg (Giacomazzo et al. 2015).

As first suggested by Zrake & MacFadyen (2013), if just 1 per cent of this energy, $E_0 \sim 10^{49}$ erg, is converted into photons in a relatively baryon-free volume surrounding the merger (e.g. with a mechanism similar to that responsible for giant flares in magnetars; see e.g. Thompson & Duncan 1995), a fireball initially dominated by electron–positron pairs can form and produce a short, high-energy transient.

From this point on, the evolution resembles that of the classical, standard *isotropic* fireball of gamma-ray bursts: the fireball accelerates to relativistic speed, up to some saturation radius $R_{\rm a}$ where the bulk kinetic energy becomes of the same order as the initial internal energy. Thereafter, the fireball coasts with a constant velocity. At some point, the transparency radius $R_{\rm t}$ is reached, after which the fireball can release radiation.

The origin of the emission is still a controversial issue in the field of GRBs. On one hand, the release of 'relic' thermal photons (i.e. the photons that constituted the initial source of pressure of the fireball, diluted by the expansion) at the transparency (photospheric) radius is expected (Meszaros & Rees 2000). On the other hand, in the case of GRBs the observed spectra suggest a non-thermal origin of the radiation, which could be the result of internal shocks (Rees & Meszaros 1994) or reconnection of the carried magnetic field (Thompson 1994) transforming part of the kinetic energy of the fireball back into radiation.

These processes may be present in our isotropic case as well, but let us first consider the thermal photospheric radiation.

The temperature of the initial blackbody can be estimated by equating the energy density of photons to that of the source magnetic field, i.e. $aT_0^4 \sim B^2/(8\pi)$, giving $T_0 \sim 4.8 \times 10^{10} B_{15}^{1/2}$ K. The acceleration ends when the bulk Lorentz factor equals $E_0/(Mc^2)$, i.e. when $\Gamma \sim 11\,E_{0,\,49}/M_{27}$ (here and in what follows, we employ the usual notation $Q_x \equiv Q/10^x$ in cgs units). This occurs at $R_{\rm a} = \Gamma R_0$, and there the comoving temperature is $T'_{\rm a} = T_0(R_0/R_{\rm a})$. Beyond $R_{\rm a}$, the temperature decreases as $T' = (R/R_{\rm a})^{-2/3}$ and Γ is constant. During these phases, the main radiative processes (pair creation and annihilation, and Compton scatterings) conserve the number of blackbody photons. This implies that the total energy contained in this 'fossil' thermal component is

$$E_{\rm BB}(R_{\rm t}) \approx E_0\,\Gamma\,\frac{T'(R_{\rm t})}{T_0} = E_0 \left[\frac{R_{\rm t}}{R_{\rm a}}\right]^{-2/3}. \quad (2)$$

The transparency radius depends on the thickness of the fireball (Daigne & Mochkovitch 2002). In our case, the fireball is thin ($R_{\rm t} \gg 2\Gamma^2 c t_{\rm inj}$) and $R_{\rm t}$ is given by (see equation 15 of Daigne & Mochkovitch 2002)

$$R_{\rm t} = \left[\frac{\sigma_{\rm T} E_0}{4\pi m_{\rm p} c^2 \Gamma}\right]^{1/2} \sim 5.9 \times 10^{12} \left[\frac{E_{0,49}}{\Gamma_1}\right]^{1/2}\,{\rm cm}. \quad (3)$$

In this case, the final blackbody energy (equation 2) can be written in terms of the two variables E_0 and M:

$$E_{\rm BB}(R_{\rm t}) = \frac{E_0}{M}\left[\frac{E_0 R_0}{c^2}\right]^{2/3}\left[\frac{4\pi m_{\rm p}}{\sigma_{\rm T}}\right]^{1/3} \sim 4 \times 10^{45}\,\frac{E_{0,49}}{M_{27}}\,(E_{0,49} R_{0,6})^{2/3}\,{\rm erg}. \quad (4)$$

With the fiducial values of the parameters, this emission is a very small fraction of the initial energy. As discussed above, there can be another mechanism able to convert a larger fraction of the bulk kinetic energy into radiation, just as in GRBs. Since there is no general consensus about this process, we leave it unspecified. This ignorance is enucleated in the efficiency parameter η, such that the energy released in this additional, non-thermal component is

$$E_\gamma = \eta E_0. \quad (5)$$

With $\eta = 10^{-2}\eta_{-2}$, we have $E_\gamma = 10^{47}\eta_{-2}E_{0,\,49}$ erg. Assuming a limiting sensitivity of 10^{-7} erg cm^{-2}, such a fireball can be detected up to a distance of $\sim$90 Mpc, close to the current horizon of LIGO/Virgo. This holds assuming that most of the EM radiation

falls into the observed band of the current instruments (i.e. between 10 and 1000 keV). This requires a radiation mechanism not only able to transform a fraction $\eta \gtrsim 10^{-2}$ of E_0 into radiation, but also able to do that in the hard X-rays. Quasi thermal Comptonization and/or synchrotron emission are the first candidates, as they are in 'standard' GRBs.

2.1 Delay and pulse duration

A point not always appreciated, in the GRB standard fireball theory, is that the delay time between the initial formation and the arrival of the fireball at the transparency radius R_t is equal to the duration of the pulse, if the fireball is thin (namely its width $\Delta R \ll R_{t)}$.

Indeed, for a thin fireball the pulse duration is comparable to the angular time-scale

$$t_{\rm ang} = \frac{R_t}{2c\Gamma^2} \sim 1 \frac{E_{0,49}^{1/2}}{\Gamma_1^{5/2}} \, {\rm s}. \quad (6)$$

The delay with respect to the initial formation, on the other hand, is given by

$$\Delta t_{\rm delay} = \frac{R_t}{c}(1-\beta) = \frac{R_t}{2c\Gamma^2}. \quad (7)$$

The two time-scales are exactly equal. In general, in GRBs the delay time is not measurable, but in the case of the detection of GWs, it can be taken as the time difference $\Delta t_{\rm delay}$ between the merger and the arrival of the first photons of the prompt.

2.2 Afterglow

After having produced the prompt emission, the fireball coasts up to the deceleration radius $R_{\rm dec}$, where it collects enough matter of the ISM to start to decelerate. The bolometric light curve corresponding to the interaction of the fireball with the ISM is characterized by a rising $\propto t^2$ phase during the coasting, and a subsequent decay as Γ decreases (Nava et al. 2013). The deceleration *onset time* $t_{\rm on}$ is given by (see Nava et al. 2013, homogeneous case)

$$t_{\rm on} = 0.48 \left[\frac{E_0}{n_0 m_p c^5 \Gamma^8}\right]^{1/3} {\rm s} = 6.5 \times 10^4 \left[\frac{E_{0,49}}{n_{0,-3}\Gamma_1^8}\right]^{1/3} {\rm s}. \quad (8)$$

This corresponds to 0.75 d. If $\Gamma = 5$, $t_{\rm on} \sim 5$ d.

3 COMPARISON OF THE AFTERGLOW EMISSION FROM THE THREE SCENARIOS

It is instructive to compare the afterglow of the isotropic fireball with the other competing models able to explain the prompt emission of sub-energetic short GRBs. As mentioned in the introduction, we have the quasi-isotropic cocoon model by Lazzati et al. (2017b, 2017a) which is essentially equivalent to the structured jet model (e.g. Kathirgamaraju et al. 2017). To this, we add what we call the off-beam slow jet, namely a rather weak and homogeneous jet, with moderate Γ, seen off-beam. In order to describe the general behaviour of the afterglow in the three scenarios, we construct example light curves with what we think are representative parameters. For all models, we use the same microphysical parameters (see Table 1), and we assume that the number density of ISM is constant and equal for all models. For definiteness, we locate the source at a luminosity distance $d_L = 60$ Mpc which is comparable to the LIGO interferometer network range at the end of the O1 observing run (Abbott et al. 2016) and represents a conservative estimate of the range during O2. This is also the limiting distance at which a strong magnetar giant flare as the one described in Lazzati et al. (2005) (which we take as a prototype for our isotropic fireball scenario) can be detected by a *Fermi*-like instrument, assuming a limiting fluence of 10^{-7} erg cm^{-2}. We compute the light curves of the jetted components with the public code `BOXFIT` (van Eerten, van der Horst & MacFadyen 2012), and those of the isotropic component with `SPHEREFIT` (Leventis et al. 2012). Since neither code accounts for the dynamics before the deceleration time, we effectively correct the light curves by smoothly joining, at the peak time given by equation (8), a power law rising as t^2 at all frequencies (Sari & Piran 1999).

Table 1. Parameters used for the models are shown in Fig. 1. For all models, we assumed an ISM number density $n_0 = 10^{-3}$ cm^{-3} and microphysical parameters $p = 2.3$, $\epsilon_e = 0.1$, $\epsilon_B = 0.01$. The source is located at a luminosity distance of 60 Mpc.

Model	$E_{\rm k,\,iso}$ (erg)	Γ	$\theta_{\rm jet}$ (deg)	$\theta_{\rm view}$ (deg)
Isotropic fireball	10^{49}	5	–	–
Spine	10^{52}	100	10	30
Layer	10^{49}	5	30	30
Off–beam	10^{51}	10	10	30

3.1 Isotropic fireball

Fig. 1 shows (left-hand panel) the predicted afterglow (in the radio, optical and X-rays) of the isotropic fireball. The onset time is close to 5 d, after which the flux decays as a power law. If a jet is not present, this is all we see. If there is a jet with standard parameters (middle panel), it becomes visible at later times ($\sim$ 100 d), when it has slowed down so that $1/\Gamma \gtrsim (\theta_{\rm view} - \theta_{\rm jet})$, i.e. when we start to see its border. Its emission in the optical and X-rays depends on the uncertain presence, at later times, of very high energy electrons. Emission in the radio, instead, is more secure. This late emission can be used as a diagnostic to distinguish between the jet-less, isotropic fireball scenario and the cocoon model by Lazzati et al. (2017a), which has similar features, but requires the presence of a jet.

3.2 Jet plus cocoon

Recently, a structured jet model (i.e. a jet with both Γ and luminosity per unit solid angle decreasing with the angular distance from the jet axis) has been proposed to describe SGRB jets when seen off-axis (Kathirgamaraju et al. 2017). To our understanding, the mildly relativistic layer/sheath found there is essentially the same structure as the cocoon described in Lazzati et al. (2017b). In this work, we thus consider the core-layer and the jet-plus-cocoon scenarios as equivalent. The middle panel of Fig. 1 mimics the expected afterglow from this scenario, obtained by summing the emission from a fast, narrow jet and that from a slower, wider jet, which represents the layer or the cocoon (parameters in Table 1). Since the latter has a wider half-opening angle, it is more likely seen within its beam. The layer afterglow peaks earlier ($\sim$5 d for the chosen parameters, which are the same as for the isotropic fireball), with the spine contributing after $\sim$100 d. As studied in Rossi et al. (2004), in this case a rather strong linear polarization should be present around

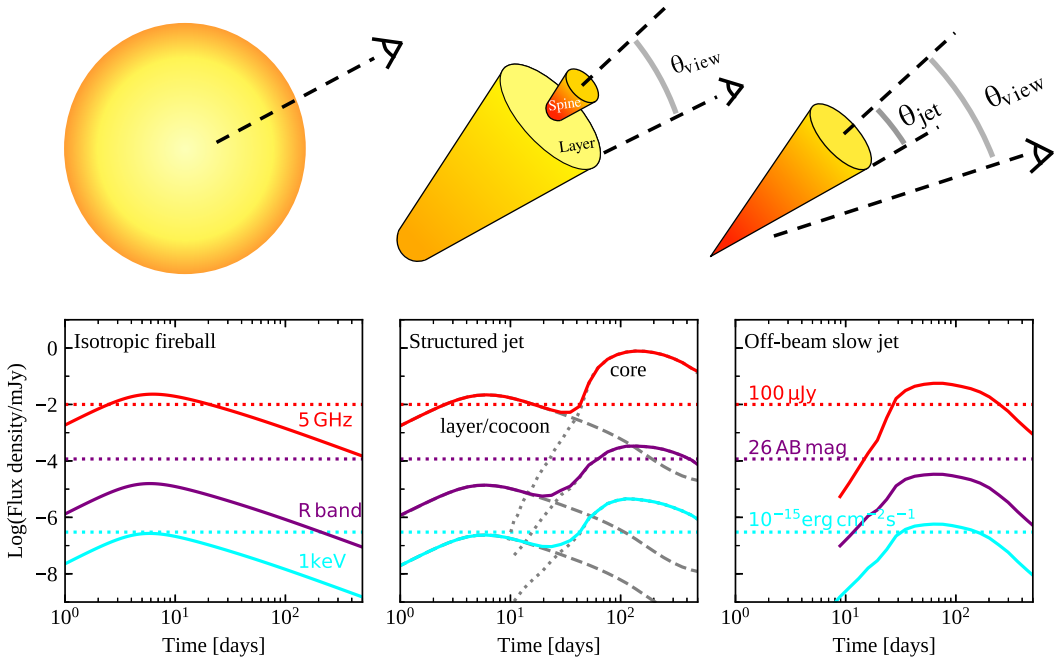

Figure 1. Indicative afterglow light curves in radio (5 GHz), optical (R band) and X-ray (1 keV) for the three scenarios. Parameters in Table 1. Left-hand panel: isotropic fireball. Mid panel: the spine/layer model (which we consider equivalent also to the jet plus cocoon scenario), where the spine is the assumed to have parameters typical of a standard SGRB jet. The layer contributes to the light curve at early times, since $\theta_{\rm layer} = \theta_{\rm view} = 30^\circ$. Right-hand panel: off-beam slow jet model. The dotted lines show representative detection limits for the three bands. The corresponding flux values are shown on the figure. The optical and X-ray fluxes are uncertain, since they depend on the presence of high energy electrons. For all models, the behaviour of the light curve is almost the same regardless of the observer frequency: this is due to all three frequencies being between $\nu_{\rm m}$ and $\nu_{\rm c}$ (for the chosen parameters) at all times shown on the plot, except for the early rising part of the off-beam slow jet and of the core.

the time when the light curve peaks, in contrast with the isotropic fireball scenario. This can be used as a diagnostic.

3.3 Off-beam slow jet

The energy distribution of SGRB jets may have a low energy tail, accompanied by a corresponding low Γ tail. In this case, a jet with $\theta_{\rm jet} \sim 10^\circ$, $E_{\rm k,\,iso} \sim 10^{51}$ erg and $\Gamma \sim$5–15 could be seen also at a relatively large $\theta_{\rm view} \sim 30^\circ$. If seen on-axis, such a jet would produce $E_{\gamma,\,\rm iso} = \eta E_{\rm k,\,iso} = 10^{50}\eta_{-1}E_{\rm k,\,iso,\,51}$ erg. These values of $E_{\rm k,\,iso}$ and Γ are roughly consistent (i.e. they are within the rather large dispersion) with the relation shown in Ghirlanda et al. (2012) and Liang et al. (2013). Using equations (2) and (3) in Ghisellini et al. (2006), we can calculate the observed $E_{\gamma,\,\rm iso}$ for any $\theta_{\rm view}$. It turns out that for $\theta_{\rm view} = 30^\circ$, the de-beaming factor is 1/2500, and then $E_{\gamma,\,\rm iso}(30^\circ) \approx 4 \times 10^{46}\eta_{-1}E_{\rm k,\,iso,\,51}$ erg, detectable up to ∼60 Mpc if the fluence limit is 10^{-7} erg cm^{-2}. For $\theta_{\rm view} > 30^\circ$, the de-beaming makes the source undetectable. The probability to see a burst within 30° is $P = (1 - \cos 30^\circ) \sim 0.13$: small, but not impossible. Taking into account the anisotropy of the GW emission (Schutz 2011), the probability to see the jet within 30° *after the progenitor NS–NS binary has been detected in GW* is significantly larger,[1] being ∼ 0.38. With the parameters listed in Table 1, we calculated the expected afterglow, shown in the right-hand panel of Fig. 1. The peak flux corresponds approximately to the time when the Lorentz factor $1/\Gamma \sim (\theta_{\rm view} - \theta_{\rm jet})$, namely when we start to see the border of the jet. This occurs at $t_{\rm peak} \sim 60$ d for the parameters shown in Tab. 1, and it goes as $t_{\rm peak} \propto (E_{\rm k,\,iso}/n_0)^{1/3}$ for a given viewing angle, i.e. it is independent from the initial Lorentz factor, due to the self-similar nature of the deceleration (Blandford & McKee 1976).

After $t_{\rm peak}$, the flux decreases monotonically. After the peak, the light curve is similar to an isotropic fireball with the same $E_{\rm k,\,iso}$ and initial Γ. However, there is an important difference: the flux of an off-beam jet should be strongly polarized at $t_{\rm peak}$, because the observer sees only the border of the jet (Rossi et al. 2004).

[1] This relies upon the assumption that the jet is launched perpendicular to the orbital plane of the binary. This most likely holds in NS–NS mergers, while it is less certain for BH–NS mergers, because the BH spin might cause the accretion disc plane in the post-merger phase to be tilted with respect to the original orbital plane.

4 DISCUSSION

Most models that associate a detectable high-energy, prompt EM counterpart to a GW event require the presence of a jet. For such counterpart to be detectable at large viewing angles, the jet must be structured, or it must be relatively slow (in order for the emission not to be too de-beamed). It can also be a standard jet, but it must deposit part of its energy in a cocoon that then expands quasi-isotropically.

In this work, we have explored the alternative possibility of the liberation of a fraction of the gravitational energy of the merging objects, instants before the merger. Several hints point towards the possibility that the energy required to form a fireball might reside in the amplified magnetic field. If a magnetized NS with $B \sim 10^{14}$ G can produce 10^{46}–10^{47} erg in radiation in a giant flare due to a re-configuration of its magnetic field, without dramatic consequences on its structure, we are confident that much more energy can be

liberated during the merger. This is also borne out by numerical simulations, which show that magnetic field amplification to values $B \sim 10^{15}$ G or larger is a natural feature of the merger phase. This magnetic energy may then produce an isotropic fireball, which can behave like a standard one even if its total energy (close to or larger than $E_0 \sim 10^{49}$ erg) is much smaller than the kinetic energy of a standard SGRB. With this energy (and for an efficiency $\eta \sim 10^{-2}$), the prompt emission of this fireball is above the detection threshold of the *Fermi*/GBM or the *Swift*/BAT instruments if the source is within a distance of $\lesssim 90$ Mpc, which is comparable to the current binary NS range of the LIGO/Virgo detector network.

Several conditions are required to form a jet and they are likely not always satisfied (as discussed in, e.g. Margalit et al. 2015; Just et al. 2016; Murguia-Berthier et al. 2017; Ruiz & Shapiro 2017), so that a relativistic jet is not necessarily associated to each merger. Nevertheless, our isotropic fireball scenario shows that a relatively low-luminosity gamma-ray prompt emission can be associated to a NS–NS merger even in the absence of such a jet. This implies that the observation of a high-energy prompt counterpart by itself does not necessarily point to the presence of a jet, which can instead only be revealed by late-time observation of the afterglow, possibly complemented by polarimetry.

Future detections of prompt high-energy transients associated to GW events will enable tests of these scenarios. Should a jet be always detected, it would imply that the conditions for jet production are always satisfied in the associated compact binary mergers. In turn, this has implications on the SGRB intrinsic rate, or equivalently on the SGRB typical half-opening angle, since it affects the ratio between the rate of SGRBs that we see on-axis and the total rate of NS–NS (or BH–NS) events (Ghirlanda et al. 2016). Until around 100 d, the afterglow of the isotropic fireball and that of the quasi-isotropic cocoon of Lazzati et al. (2017a) should be very similar, if they start with a comparable E_0 and Γ. What distinguishes them is mainly the presence or absence of a 'standard' jet. If the cocoon is much less isotropic, as seems to be the case (Lazzati et al. 2017b), its afterglow may have an earlier onset, and it should show polarization at all frequencies also at early times (close to the cocoon onset time). The same should occur also for the off-beam slow jet, which should show polarization close to the peak time, when the emission is dominated by the jet border. To conclude, we would like to stress that the possibility to have a prompt and an afterglow emission even without a jet has far reaching consequences on the search for the EM counterparts to GW events, on the physics itself of the merger, and on the typical aperture angle of the jets of SGRBs.

ACKNOWLEDGEMENTS

We are grateful to Monica Colpi and Albino Perego for useful discussions.

REFERENCES

Abbott B. P. et al., 2016, Living Rev. Relativ., 19, 1
Berger E., 2014, ARA&A, 52, 43
Blandford R. D., McKee C. F., 1976, Phys. Fluids, 19, 1130
D'Avanzo P. et al., 2014, MNRAS, 442, 2342
Daigne F., Mochkovitch R., 2002, MNRAS, 336, 1271
Ghirlanda G., Nava L., Ghisellini G., Celotti A., Burlon D., Covino S., Melandri A., 2012, MNRAS, 420, 483
Ghirlanda G. et al., 2016, A&A, 594, A84
Ghisellini G., Ghirlanda G., Mereghetti S., Bosnjak Z., Tavecchio F., Firmani C., 2006, MNRAS, 372, 1699
Giacomazzo B., Zrake J., Duffell P. C., MacFadyen A. I., Perna R., 2015, ApJ, 809, 39
Gottlieb O., Nakar E., Piran T., 2018, MNRAS, 473, 576
Hurley K. et al., 2005, Nature, 434, 1098
Just O., Obergaulinger M., Janka H.-T., Bauswein A., Schwarz N., 2016, ApJ, 816, L30
Kathirgamaraju A., Barniol Duran R., Giannios D., 2017, MNRAS, preprint (arXiv:1708.07488)
Kiuchi K., Kyutoku K., Sekiguchi Y., Shibata M., Wada T., 2014, Phys. Rev. D, 90, 041502
Lazzati D., Ghirlanda G., Ghisellini G., 2005, MNRAS, 362, L8
Lazzati D., Deich A., Morsony B. J., Workman J. C., 2017a, MNRAS, 471, 1652
Lazzati D., López-Cámara D., Cantiello M., Morsony B. J., Perna R., Workman J. C., 2017b, ApJ, 848, L6
Leventis K., van Eerten H. J., Meliani Z., Wijers R. A. M. J., 2012, MNRAS, 427, 1329
Liang E. -W. et al., 2013, ApJ, 774, 13
Li L.-X., Paczyński B., 1998, ApJ, 507, L59
Loeb A., 2016, ApJ, 819, L21
Margalit B., Metzger B. D., Beloborodov A. M., 2015, Phys. Rev. Lett., 115, 171101
Meszaros P., Rees M. J., 2000, ApJ, 530, 292
Metzger B. D., 2017, Living Rev. Relativ., 20, 3
Murguia-Berthier A. et al., 2017, ApJ, 835, L34
Nava L., Sironi L., Ghisellini G., Celotti A., Ghirlanda G., 2013, MNRAS, 433, 2107
Perna R., Lazzati D., Giacomazzo B., 2016, ApJ, 821, L18
Pescalli A., Ghirlanda G., Salafia O. S., Ghisellini G., Nappo F., Salvaterra R., 2015, MNRAS, 447, 1911
Price D. J., 2006, Science, 312, 719
Rees M. J., Meszaros P., 1994, Astrophys. J. Lett., 430, L93
Rossi E. M., Lazzati D., Salmonson J. D., Ghisellini G., 2004, MNRAS, 354, 86
Ruiz M., Shapiro S. L., 2017, Phys. Rev. D, 96, 084063
Salafia O. S., Ghisellini G., Pescalli A., Ghirlanda G., Nappo F., 2015, MNRAS, 450, 3549
Sari R., Piran T., 1999, ApJ, 520, 641
Schutz B. F., 2011, Class. Quantum Gravity, 28, 125023
Thompson C., 1994, MNRAS, 270, 480
Thompson C., Duncan R. C., 1995, MNRAS, 275, 255
Troja E. et al., 2016, ApJ, 827, 102
van Eerten H., van der Horst A., MacFadyen A., 2012, ApJ, 749, 44
Yamazaki R., Asano K., Ohira Y., 2016, Progress of Theoretical and Experimental Physics, 2016, 051E01
Zrake J., MacFadyen A. I., 2013, ApJ, 769, L29

This paper has been typeset from a TEX/LATEX file prepared by the author.